Natural Resources Research, Vol. 16, No. 3, September 2007 (© 2007)
DOI: 10.1007/s11053-007-9050-9

Frequency Distribution of Thickness of Sediments Bounded by Cenozoic Biostratigraphic Events in Wells Drilled Offshore Norway and along the Northwestern Atlantic Margin

Frits Agterberg,[1,2,5] Felix Gradstein,[3] and Gang Liu[2,4]

Received 1 June 2007; accepted 1 June 2007
Published online: 17 August 2007

Sampling for microfossils in exploratory wells in basins with hydrocarbon potential is subject to considerable uncertainty, mainly because the samples usually are small and subject to caving. Biostratigraphic events defined on fossil taxa include their last occurrences of which the depths along the wells generally can be measured with precision. The RASC method for ranking and scaling of stratigraphic events produces an average basin-wide optimum sequence and zonation that can be used for correlation of strata between wells. In this optimum sequence the fossil events are ordered according to their occurrences in geological time. Depth differences between successive events in the optimum sequence satisfy a frequency distribution that is of interest for potentially increasing stratigraphic resolution. In this article the depth difference frequency distribution is modeled for three large Cenozoic microfossil data sets consisting of 30 wells in the North Sea Basin, 27 wells on the Labrador Shelf and Grand Banks, and 11 wells in the western Barents Sea. The shapes of the three frequency distributions satisfy bilateral gamma distributions with similar parameters. These distributions are fitted by the construction of straightlines on normal Q–Q plots of square root transformed average-corrected depth differences. The gamma distribution model is approximately satisfied except for small negative and positive depth differences, which have anomalous frequencies because of the discrete sampling method used in exploratory well-drilling to collect microfossils. It implies not only comparable average stratigraphic order of events, but also comparable average sedimentation rates in the three Cenozoic basins selected for study.

KEY WORDS: Sediment thickness, biostratigraphic events, exploratory wells, bilateral gamma distribution, normal Q–Q plots, North Sea Basin, Northwestern Atlantic Margin.

INTRODUCTION

Quantitative methods for the analysis of observed biostratigraphic events include the RASC method for ranking and scaling (Agterberg and Gradstein, 1999). Development phases for this approach were:

(1) 1978–1985: Starting from an algorithm for ordering biostratigraphic events proposed by Hay (1972), the basic concepts of RASC were introduced and applied initially to Cenozoic Foraminifera in offshore wells drilled along the northwestern Atlantic Margin (Gradstein and Agterberg, 1982). Implementation of the method was in the form of mainframe computer

[1]Geological Survey of Canada, 601 Booth Street, Ottawa ON, Canada K1A0E8.
[2]University of Ottawa, Ottawa ON, Canada K1N6N5.
[3]Geological Museum, University of Oslo, PO Box 1172, Blindern, Oslo N-0318, Norway.
[4]State Key Laboratory of Geological Processes and Mineral Resources, China University of Geosciences, Wuhan 430074, China.
[5]To whom correspondence should be addressed; e-mail: agterber@nrcan.gc.ca

programs (Agterberg and Nel, 1982a, b; Agterberg and others, 1985). Development of RASC was carried out at the Geological Survey of Canada in Ottawa and Halifax, Nova Scotia, as part of Project 148 of the International Geological Program (Evaluation and Development of Quantitative Stratigraphic Correlation Methods, 1976–1985; cf. Gradstein and others, 1985).

(2) 1986–1994: Minor modifications of the method were introduced (Agterberg and Gradstein, 1988; D'Iorio and Agterberg, 1989; Agterberg, 1990) followed by new types of applications by Williamson (1987), Van Buggenum (1991), Gradstein and others (1992), Schioeler and Wilson (1993), and Gradstein and others (1994). Implementation was in form of programs for personal computers (Agterberg and others, 1989).

(3) 1995–2005: Modifications of RASC with addition of variance analysis were presented in Agterberg and Gradstein (1997, 1999), and Gradstein and Agterberg (1998). This stage of development was sponsored by Saga Petroleum with applications to Cretaceous and Cenozoic microfossils from wells drilled in the North Sea Basin offshore Norway. RASC has had large-scale applications by other oil companies including Unocal, Shell, Arco, British Petroleum, North Hydro, Chevron, and British Gas. Novel applications included Gradstein and Bäckström (1996), Whang and Zhou (1997), and Pawlowsky-Glahn and Egozcue (2001). A user-friendly Windows version of RASC was developed (Agterberg, Gradstein, and Cheng, 1998, 2001) to complement and replace the earlier mainframe and DOS versions.

(4) 2006-present: Currently, the Windows version of RASC is being extended primarily to improve its CASC component for correlation and standard error calculation using the observed depths of biostratigraphic events in the wells. The three data sets used in this new development are Cenozoic microfossils in (A) 30 North Sea wells, using 1430 event records of 289 taxa of benthic and planktonic Foraminifera, some miscellaneous shelly microfossils, and dinoflagellates; (B) 27 Labrador Shelf-northern Grand Banks wells, using 966 event records of 178 taxa of benthic and planktonic Foraminifera, and few miscellaneous microfossils; and (C) 12 western Barents Sea wells using 625 event records of 122 taxa of agglutinated benthic Foraminifera, and dinoflagellates. These three data sets were analyzed previously by RASC and CASC. Results for data sets (A) and (C) were summarized in Kaminski and Gradstein (2005) and data set (B) was originally used when RASC and CASC were first developed (see e.g., Gradstein and Agterberg, 1982). Gang Liu is working with us to upgrade the Windows version of RASC/CASC (to be named RASCW later in this article) and develop graphic routines for depth scaling (Liu, Cheng, and Agterberg, in press).

DESCRIPTION OF DATA AND SUMMARY OF RASC RESULTS

Different types of stratigraphic events can be defined for the same fossil taxon. Its first and last occurrences are most frequently used. Other events such as first consistent occurrence, peak occurrence, and last consistent occurrence can be used occasionally. The vast majority of events in our data sets are last occurrences of which the depths in wells could be measured precisely, without contamination of well samples by stratigraphically younger material. An example of events as observed in one of the wells of data set (A) is shown in Table 1. Although microfossil taxa were observed in nearly all samples that were taken when a well was drilled, most samples did not show any observable events for these taxa; on the other hand, some samples produced more than one observed event for two or more taxa.

Figure 1, which was obtained by use of RASCW, shows frequency distributions of all events in each of the three data sets. These cumulative frequency curves are 'hollow' because relatively many events were observed in one or a few wells only, and few or no events were observed in all wells. An important input parameter for RASC is k_c representing minimum number of wells in which an event was observed to occur. The main reason for setting k_c is that RASC computes average positions for

Table 1. First 28 Fossil Events in order of Ranked Optimum Sequence for WELL # 18 of Data Set (A): Esso (N) 16(1–1); Events are Last Occurrences Except for a Single Last Common Occurrence (LCO) and Two Log Markers

#	Sequence #	Depth (m)	Event #	Event Name
1	1	381	77	*Elphidium* spp.
2	2	381	228	*Cassidulina teretis*
3	4	637	1	*Neogloboquadrina pachyderma*
4	7	381	270	*Cibicidoides grossa*
5	9	637	4	*Globorotalia inflata*
6	13	637	23	*Sigmoilopsis schlumbergeri*
7	14	707	269	*Neogloboquadrina atlantica*
8	15	726	266	*Globorotalia puncticulata*
9	17	643	219	*Martinotiella cylindrica*
10	19	908	285	*Caucasina elongata*
11	20	822	91	Diatoms/radiolarians LCO
12	21	1036	282	*Uvigerina ex.gr. semiornata*
13	23	1128	207	NS Log G
14	24	899	125	*Neogloboquadrina continuosa*
15	25	734	71	*Epistomina elegans*
16	26	899	15	*Globigerina praebulloides*
17	28	899	236	*G. ex.gr. praescitula zealandica*
18	29	908	17	*Asterigerina gurichi*
19	34	1395	24	*Turrilina alsatica*
20	36	1219	25	Coarse agglutinated spp.
21	37	1395	97	*Cyclammina placenta*
22	38	1395	182	*Spirosigmoilinella compressa*
23	39	1584	262	*Karrerulina horrida*
24	42	1395	140	*Rotaliatina bulimoides*
25	43	1554	261	*Haplophragmoides walteri*
26	46	1554	321	*Dorothia seigliei*
27	47	1554	289	*Adercotryma agterbergi*
28	49	1531	206	NS Log F

events along a single scale that applies to the entire data set. Precision of average positions increases rapidly when k_c is increased. For most RASC runs on the three data sets, k_c was set equal to 6 (A), 7 (B), and 6 (C), respectively.

A drawback of this procedure is that events occurring in one or fewer than k_c wells would be eliminated from the data set although they can be stratigraphically important, for example their age in millions of years may be known precisely and this would help in determining the age of events in the vicinity of these rare events. Stratigraphically significant rare events that occur in fewer than k_c wells can be reintroduced by declaring them to be ''unique events.'' The positions of unique events can be estimated with reasonable precision by subsequently fitting them into the ranked and scaled optimum sequences obtained by RASC.

In addition to unique event selection, RASCW allows for the selection of ''marker horizons.'' These are events that occur in k_c or more wells with precisely known positions in the wells in which they occur. These, for example, could be ash layers, seismic events or biostratigraphic events with relatively little associated uncertainty such as planktonic flooding events. Marker horizons receive more weight than other events during scaling because their positions in the wells are assumed to be known with certainty.

In general, the main RASC output consists of both a ranked and a scaled optimum sequence. In the ranking solution the events are simply ordered according to their average successive occurrence in geological time. In the scaled optimum sequence, successive events are separated by ''interevent'' distances or intervals. These distances are computed from crossover frequencies of all event pairs, with higher crossovers resulting in smaller scaling values. Successive events with zero or small interevent distance between them belong to the same cluster of events when scaling results are represented by means of a dendrogram. Figure 2 shows ranked and scaled optimum sequence for data set (A). Events with names preceded by two asterisks in Figure 2 are unique events. For this example, k_c was set equal to 10 and log markers in data set A were selected as

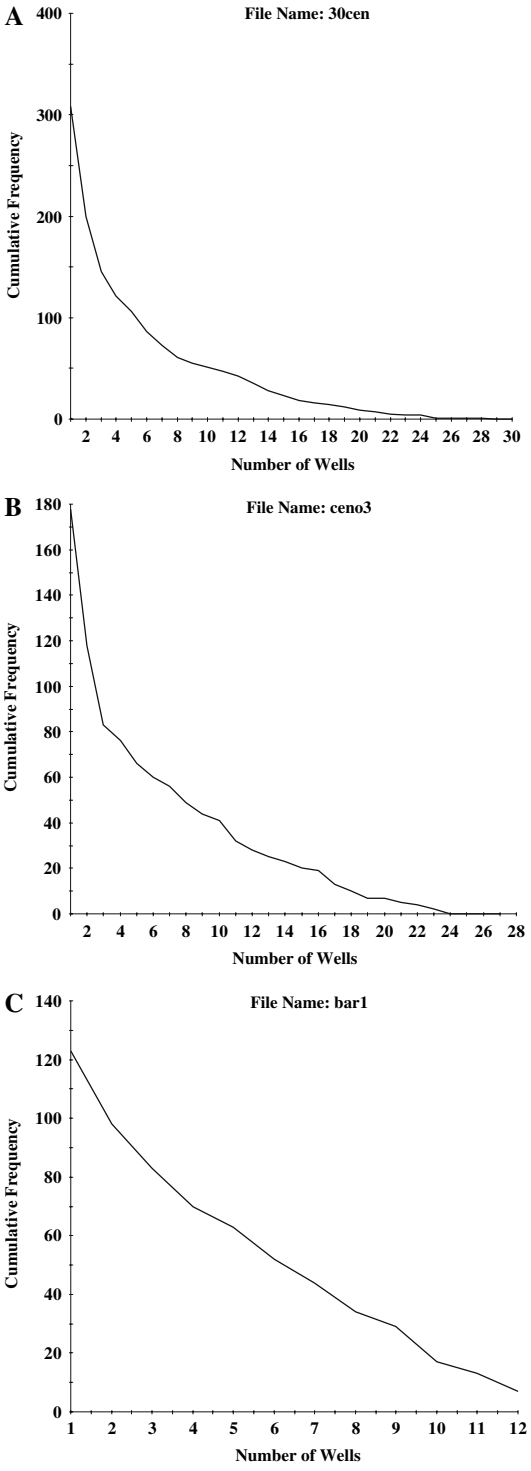

Figure 1. Cumulative fossil event frequency distributions for data sets (A), (B), and (C), respectively. Unless stated otherwise, RASC threshold parameter k_c to be used later in this article was set equal to 6, 7, and 6, for data sets (A), (B), and (C), respectively.

marker horizons (names preceded by one asterisk in scaled optimum sequence).

More details on how ranked and scaled optimum sequences are derived and their interpretation are given in Agterberg and Gradstein (1999). The following remarks are restricted to aspects relevant for this article. The first part of Figure 2 shows number (N) of wells in which an event occurs, and the event's standard deviation, which also is displayed graphically. Events with small standard deviations are relatively good markers, whereas events with large standard deviations are less useful for correlation between wells.

The standard deviation of an event is computed from deviations for it from lines of correlation constructed for all sections. An example of a line of correlation is shown in Figure 3. The vertical scale in this graph is for relative sample position in the well. In any well, the relative sample positions of events differ from those in the ranked optimum sequence. If an event falls on the line of correlation, its deviation is zero and if it nearly falls on the lines of correlation for all wells in which it occurs, the event has small standard deviation and is a good marker. The 'average' standard deviation (Well SD in Fig. 2, first part) is computed from variances of all deviations for the same event in all wells.

The order of events in the scaled optimum sequence (Fig. 2, second part) generally differs slightly from the order in the ranked optimum sequence because of minor reordering resulting from interevent distance estimation. Every interevent distance plotted in the dendrogram represents the distance between an event and the event below it. Large interevent distances are associated with breaks in the fossil record: they may indicate hiatuses at unconformities that can be interpreted in terms of sequence stratigraphy. Unique events (marked by two asterisks) are helpful for identifying the clusters in which they occur. An optimum sequence can be regarded as a composite standard zonation for the study area. Figure 4 for data set (A) after Kaminski and Gradstein (2005) is an example of a fully interpreted scaled optimum sequence.

Each of the 87 events in Figure 4 occurs in at least 7 wells, except for 15 unique events. There are 18 zones and subzones assigned, named NSR 1–13 (North Sea RASC), of early Paleocene through early Pleistocene. Large breaks (at events 129, 50, 206, 6, 266, and 23) indicate transitions between natural microfossil sequences, or hiatuses. The zones

contain 33 agglutinated benthic events (32× Last Occurrence and 1× Last Common Occurrence) for 32 taxa (Kaminski and Gradstein, 2005, p. 51). The total stratigraphic range of taxa may extend younger than the average stratigraphic range, with the result that the average last occurrences displayed in the RASC zonation may be slightly older. On average, event observation in the wells may be closer to the average stratigraphic position than the last occurrence end point of the range chart (see Kaminski and Gradstein, 2005, fig. 22).

RASC analysis can be followed by CASC analysis in which relative stratigraphic position of an event in a well is replaced by its depth (in meters or feet) in that well. Figure 5 is an example. It shows a new line of correlation, which is a transformed version of the smooth curve in Figure 2. Positions of events on these new lines of correlation are used in CASC well correlation displays. However, in this article we are not primarily concerned with correlation between wells. Emphasis is on the frequency distribution of depth differences in wells between events in these wells ordered according to the optimum sequence.

FREQUENCY DISTRIBUTIONS OF DEPTH DIFFERENCES

Figure 6 shows histograms of depth differences between successive events in all sections for each data set. The ranked optimum sequence was used and first-order depth differences were measured by subtracting the depth of an observed event from the depth of the event below it in a well. Thus the first-order depth difference is positive when the depth of

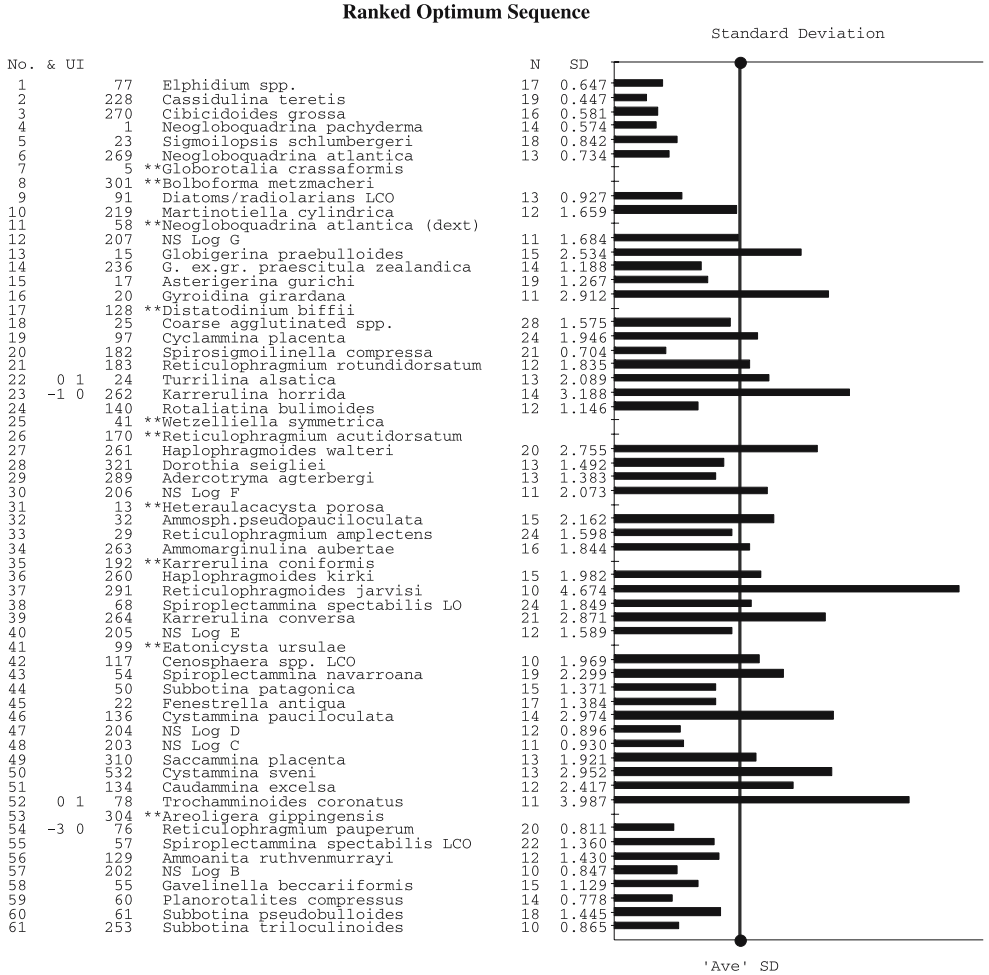

Figure 2. Ranked and scaled optimum sequence for events observed in 10 or more wells for data set (A).

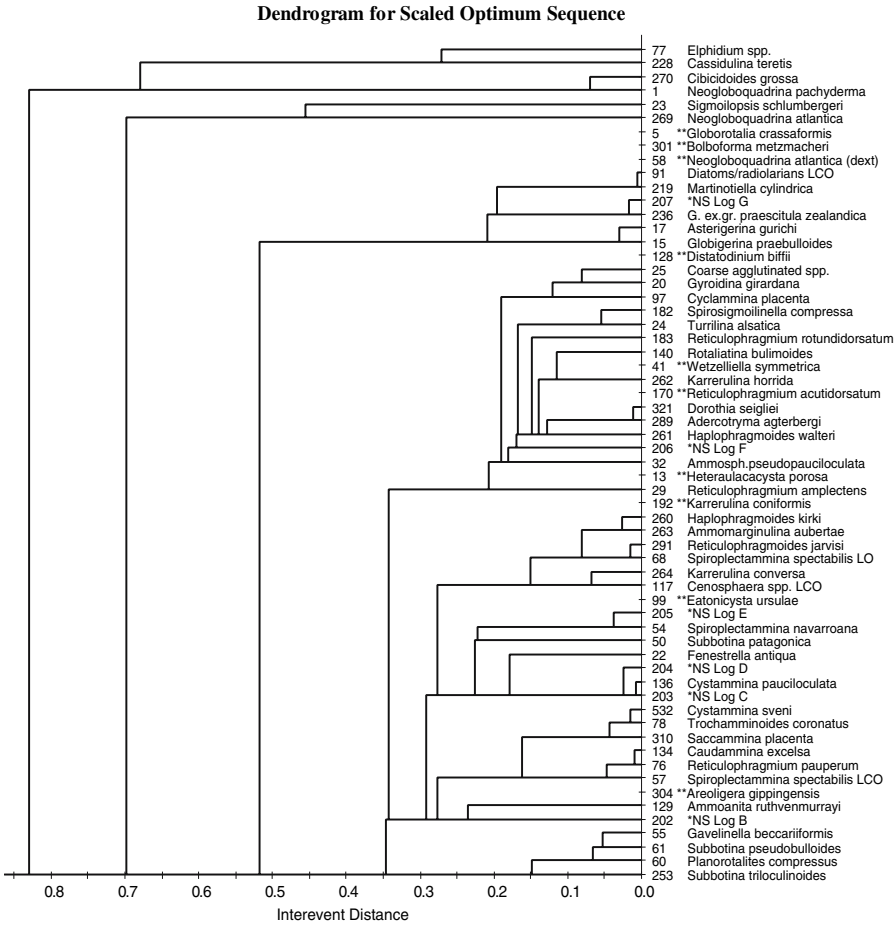

Figure 2. continued.

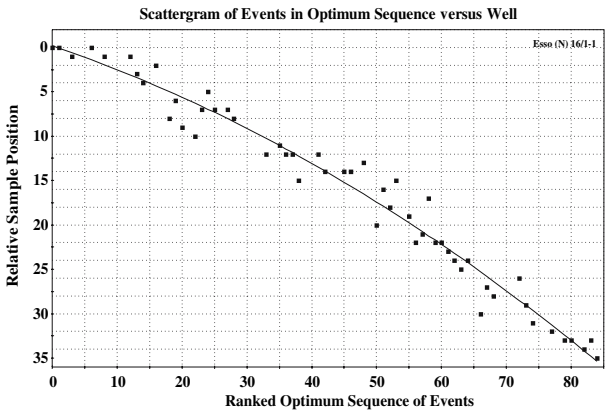

Figure 3. Ranking scattergram with line of correlation for Well # 18 in data set (A).

the event below an event is greater, and negative when it is less. Figure 5 can be used to illustrate this procedure. In general, the cluster of points for observed depths dips to the right on this graph. This reflects the fact that, on average, events that are stratigraphically lower in the optimum sequence have greater depths. A negative first-order depth difference arises when the depth of an event is less than that of its neighbor to the right in Figure 5.

The histograms of Figure 6 are similar in shape. Each underlying frequency density curve can be assumed to be symmetrical with respect to the mean value, which amounts to 45.7, 70.9, and 13.8 m for data sets (A), (B), and (C), respectively. In comparison with a normal (Gaussian) distribution, the first-order depth difference frequency distribution is more sharply peaked, and has long thin tails extending to large positive and negative values. This also is illustrated in the normal Q–Q plots of Figure 7. The shapes of the frequency distributions in Figure 7 are far from straightlines that would correspond to normal distributions.

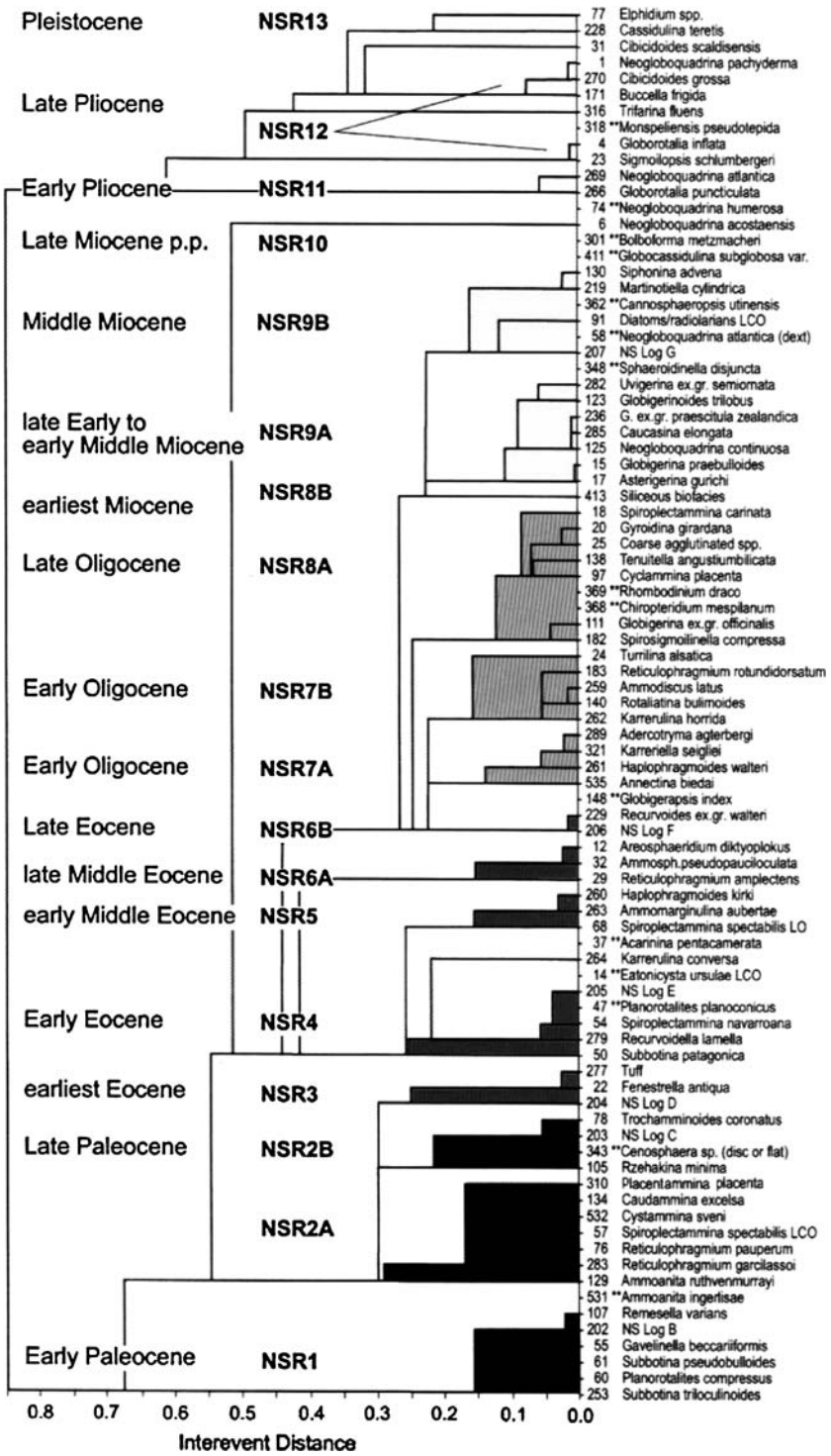

Figure 4. Scaling in relative time of the optimum sequence for events observed in 7 or more wells for data set (A) (after Kaminski and Gradstein, 2005, Fig. 18, p. 50). Eighteen NSR (North Sea RASC) zones of Paleocene through Plio-Pleistocene age originally were recognized by Gradstein and Bäckström (1996).

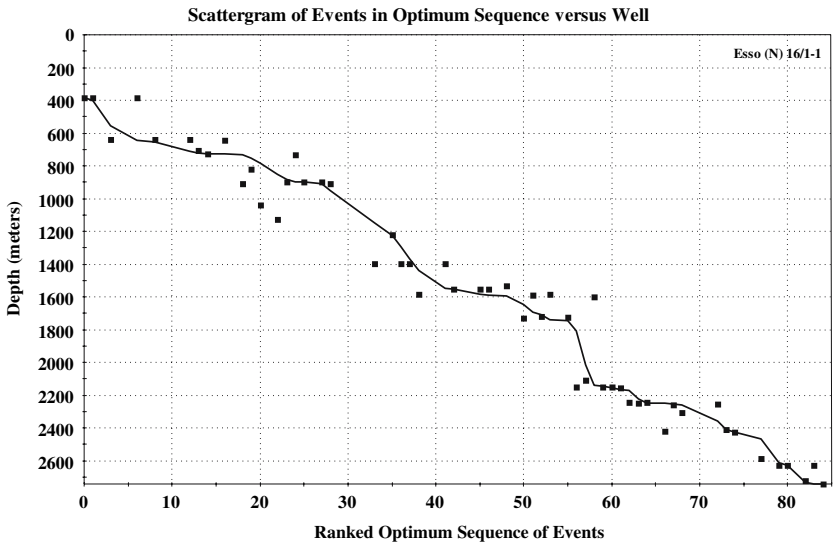

Figure 5. Depth ranking scattergram with line of correlation for Well # 18 in data set (A). Relative sample positions shown in Figure 3 have been replaced by depths of samples.

However, when the first-order depth differences are first corrected for their mean value, each frequency distribution becomes approximately normal after a square-root transformation of the following type: a positive depth difference is replaced by its square root, and a negative depth difference by a negative number with absolute value equal to the square root of the absolute value of the negative depth difference (see Fig. 8). Except for an upward bulge in the middle, and minor fluctuations in the tails, the square root and average transformed depths for each data set now show straightline patterns corresponding to normal (Gaussian) distributions.

Figure 9 is an estimate of the shape of the probability density curve of the central bulge for data set (A). It was derived from the differences between observed values and values on a base line constructed by extrapolating the straightline shown in Figure 8A into the central part underlying the upward bulge.

In general, in a data set with depths of samples taken at a regular discrete sampling interval, a number of events are observed to be coeval. Because the sampling interval is discrete and not continuous, it is likely that events that took place at nearly the same time, and occupy only slightly different points along the axis of time, would be observed to be coeval. Each frequency distribution of Figure 8 shows a vertical straightline segment on the left side of its central upward bulge. The abscissa of this vertical straightline segment is the square root transformed and average-corrected value of zero depth difference for all pairs of successive events observed to be coeval.

The straightlines shown in Figure 8 pass through the origin and were fitted by ordinary least squares using all observed depth differences except those situated on the central upward bulge. The slopes of the straightlines for data sets (A), (B), and (C) are 0.0902, 0.0746, and 0.0968, respectively. These estimates are remarkably close to one another, although the three study areas are far apart geographically. This indicates that the frequency distribution of depth differences for Cenozoic microfossils (mostly last occurrences of Foraminifera) has a distinct shape that is approximately the same for the three study areas. It implies not only comparable average stratigraphic order of events, but also comparable average sedimentation rates in the three Cenozoic basins selected for study.

In order to illustrate the plausibility of the preceding explanation that the central upward bulge is the result of sampling at a regular interval, the following two computer simulation experiments were performed: 1000 random normal numbers were generated with zero mean and standard deviation equal to 11.1 representing the standard deviation for square root transformed and average-corrected first-order depth differences in data set (A). As expected,

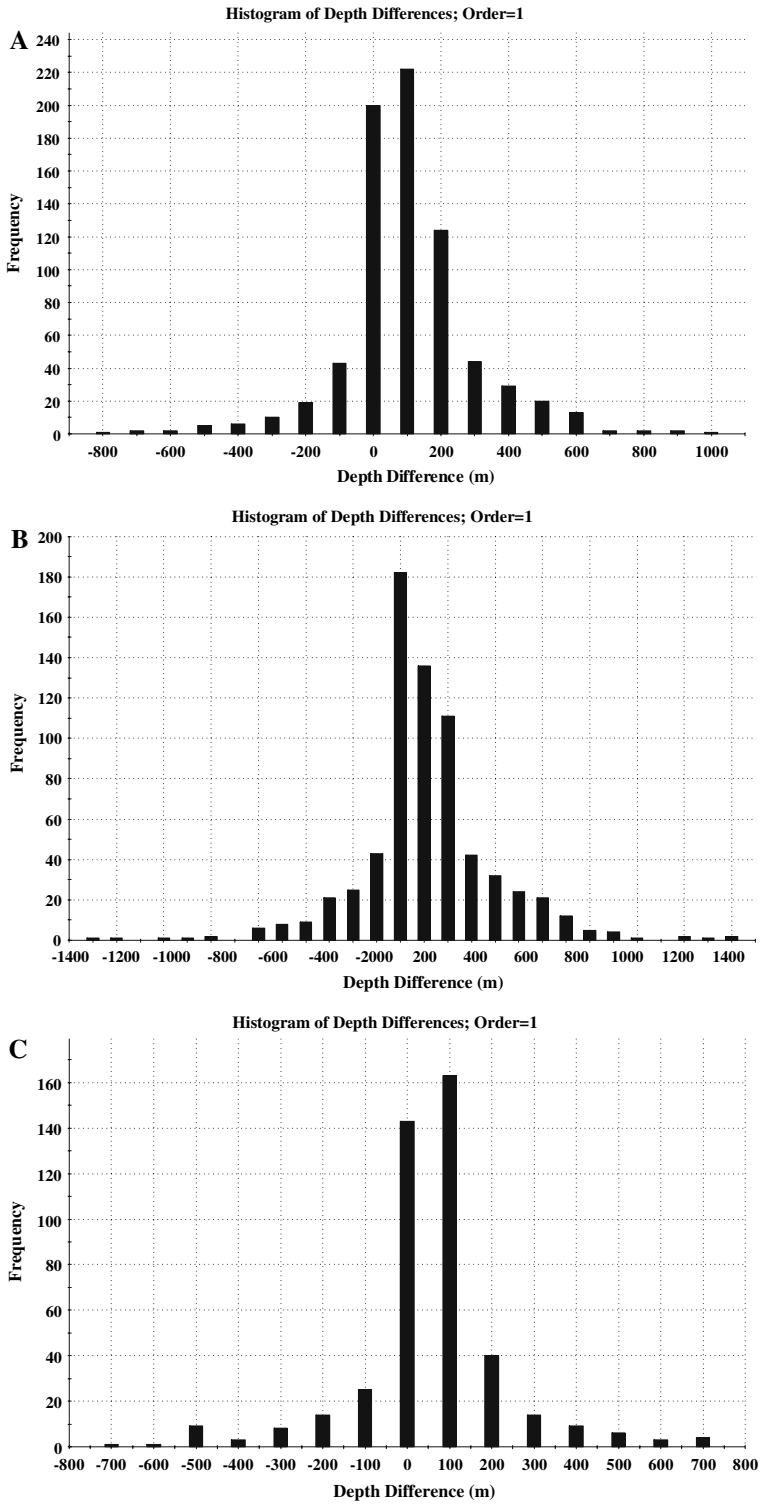

Figure 6. Histograms for first-order depth differences for data sets (A), (B), and (C), respectively.

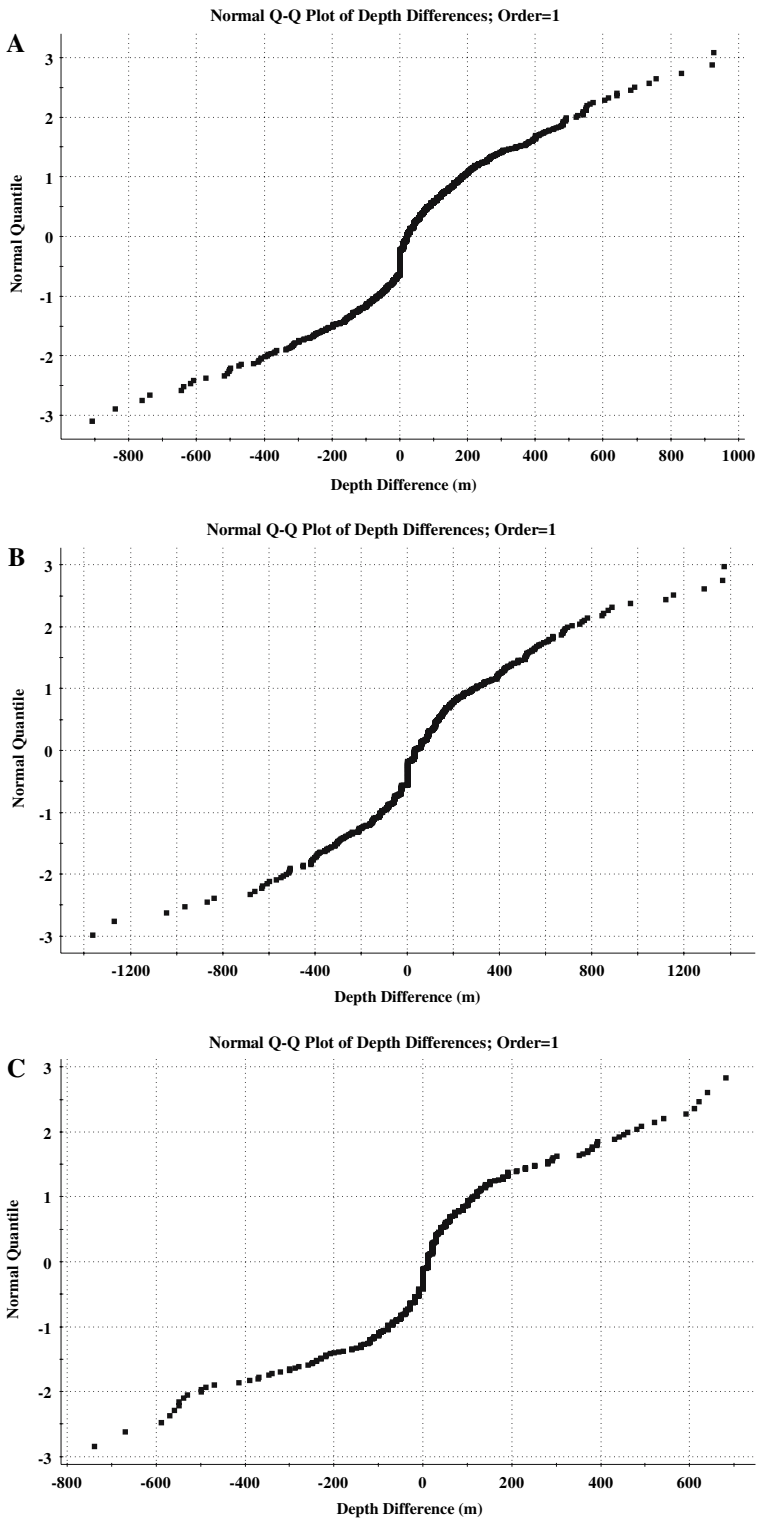

Figure 7. Normal Q–Q plots of first-order depth differences for data sets (A), (B), and (C). Because normal (Gaussian) distributions would plot as straightlines, non-normality is clearly demonstrated.

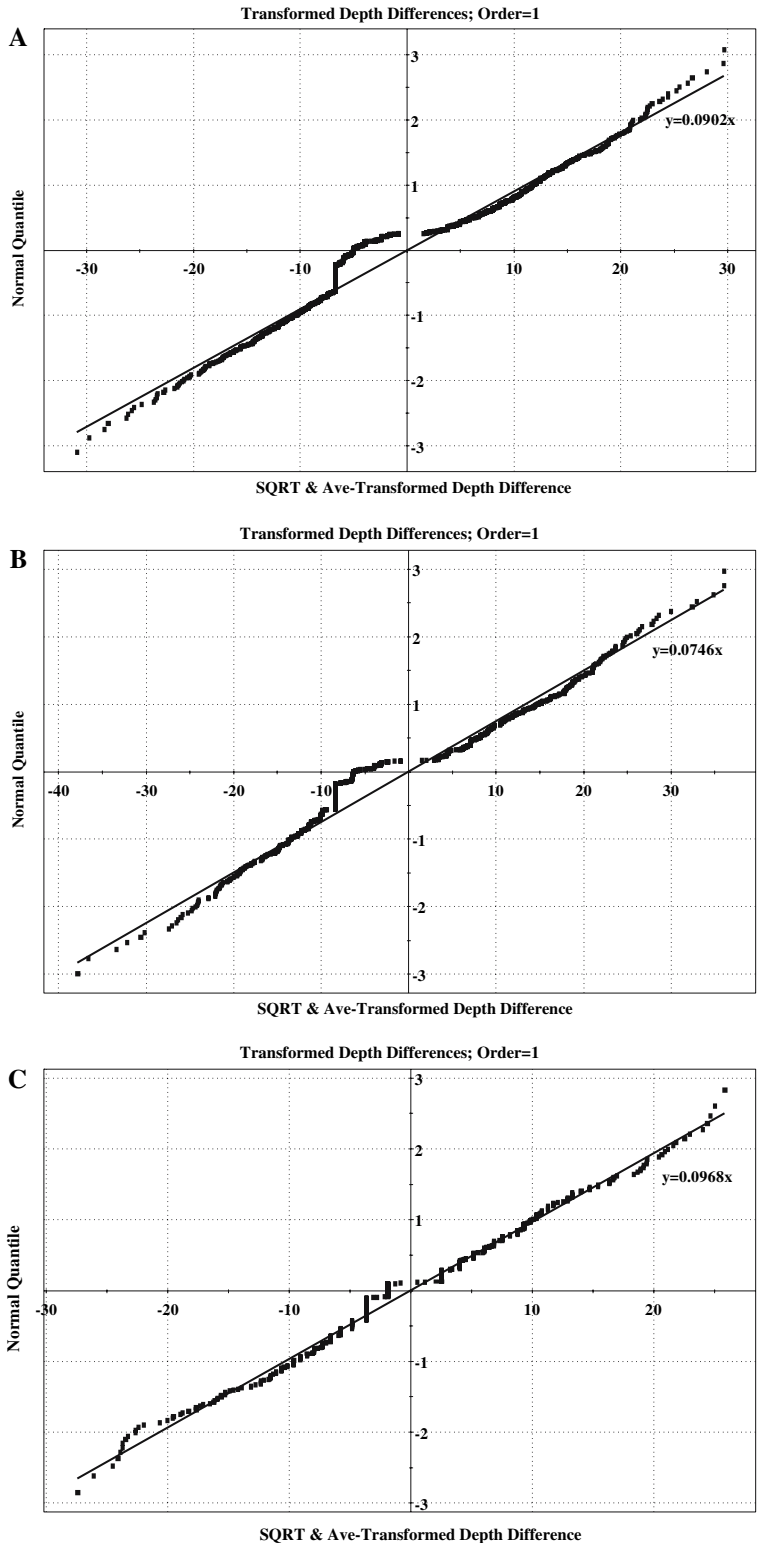

Figure 8. Normal Q–Q plots of first-order square root transformed depth differences for data sets (A), (B), and (C). Approximate normality is demonstrated except for anomalous upward bulge in center of each plot.

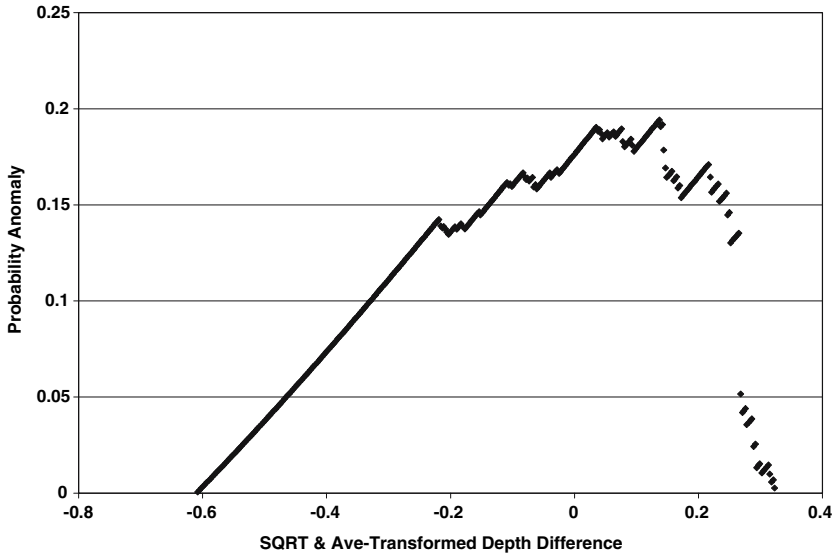

Figure 9. Frequency density plot of anomalous upward bulge in center of Figure 8A.

the two frequency distributions of these 1000 numbers plot approximately as straightlines on a normal Q–Q plot. First, all values for square root transformed depth differences between -7 and 0 were replaced by zeros. Normal quantile values corresponding to -7 and 0 are -0.64 and 0, respectively. The resulting Q–Q plot is shown in Figure 9A.

The underlying assumption for this first experiment is that, because of discrete sampling, depth differences between all events less than about 50 m apart were artificially replaced by zeros. Although Figure 10A shows a central upward bulge, the shape of this bulge is triangular and does not resemble the shapes seen in Figure 8. Clearly, the effect of discrete sampling is not spike-like but more gradational.

A more realistic picture is shown in Figure 10B for the second experiment where the base of the anomaly was assumed to extend from -7 to 3 and the range of normal quantiles from -0.64 to -0.2 (instead of from -0.64 to 0 in Fig. 9A). The standard deviation for this interval was assumed to be equal to that of the original set of random numbers (=11.1). Although the shape of the bulge in Figure 10B resembles those in Figure 6, and is more realistic than that in Figure 10A, the real situation is more complex, partly because individual biostratigraphic events have different standard deviations (cf. Fig. 2A).

Histograms and Q–Q plots also can be obtained for depth differences of orders greater than 1. Figure 11 (for data set A only) shows Q–Q plots of square root and average-transformed depth differences for pairs of events that are between 2 and 5 positions apart in the optimum sequence. The average value of k-th order depth differences is $k \times m$ where m represents the average value of first-order depth differences. The point patterns in Figure 11 are not as close to straightline patterns as the patterns in Figure 8A. Divergence from linearity increases with order of depth differences.

Widths of discrete sampling anomalies in Figure 11 are controlled by $k \times m$ instead of m where k represents order. Superpositional relations derived from higher order depth differences are used in so-called indirect inter-event distance estimation in RASC scaling (Agterberg and Gradstein, 1999). It is likely that departures from normality of square root transformed depth differences are at least partly the result of differences in rates of sedimentation that affect higher order depth differences more strongly than first-order depth differences.

DISCUSSION

Suppose that X is the random variable representing first-order depth difference corrected for its mean value. Because for the three data sets used in this article, $X^{1/2}$ satisfies a normal (Gaussian) distribution with mean μ (=0) and variance σ^2, it follows that the frequency density function of X is:

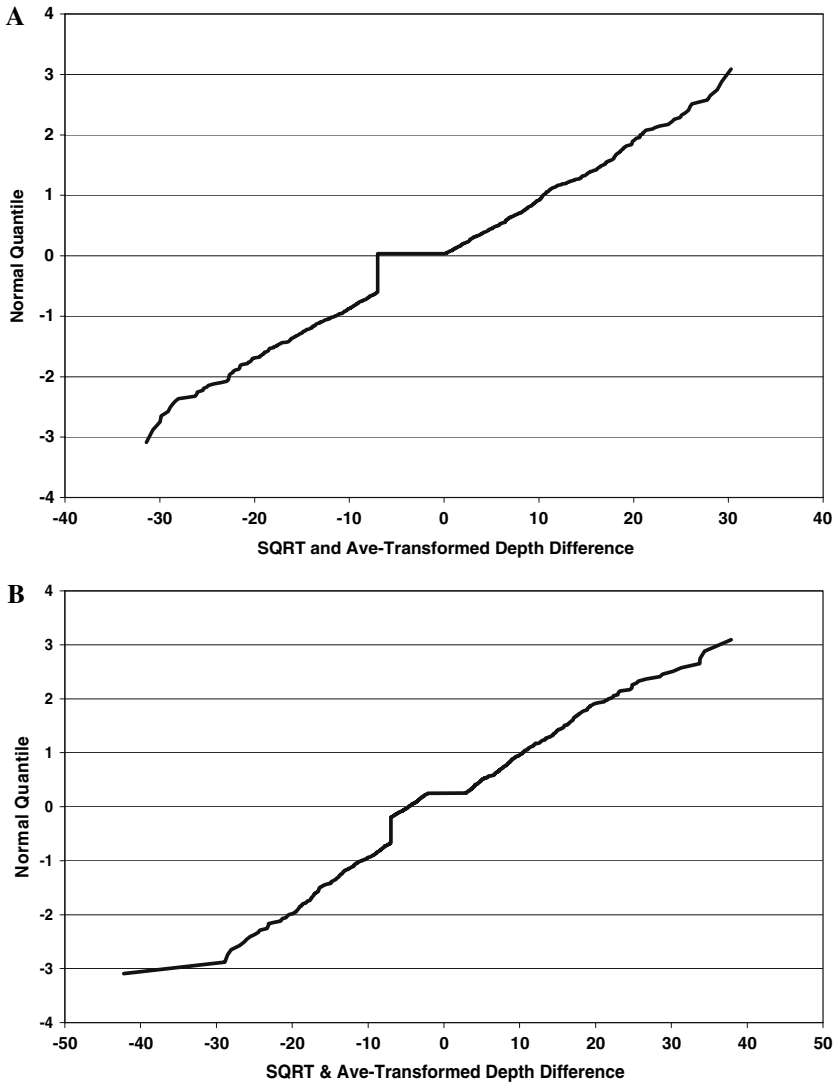

Figure 10. Normal Q–Q plots of 1000 random normal numbers in two computer simulation experiments with central anomaly resulting from discrete sampling. A, Spike-like anomaly of coeval events; B, Smoothed anomaly (see text for further explanation).

$$p_X(x) = \frac{1}{2\sqrt{\pi\beta \cdot |x|}} e^{-|x|/\beta} \qquad (1)$$

where $\beta = 2\sigma^2$. This is the equation of a double or bilateral gamma distribution. Figure 12 shows frequency density curves satisfying [Eq. (1)] for the three data sets. These continuous curves with logarithmic probability scale in the vertical direction correspond to the histograms of Figure 6. Gaussian density plots would plot as parabolas on this type of graph.

Because of the exceedingly long thin tails for both positive and negative values of X, it is difficult to use observed depth differences for scaling and correlation. For example, in a sample of 10 wells a single pair of events with depth difference of 1000 m (or -1000 m) between them could change the arithmetic average by nearly 100 m because most other pairs of events would probably have depth differences close to the relatively small mean value coinciding with the relatively sharp peak of the depth difference frequency density curve (cf. Fig. 6).

Although the nature of the frequency distribution of depth differences was not known well before the recent development of RASCW, the fact that

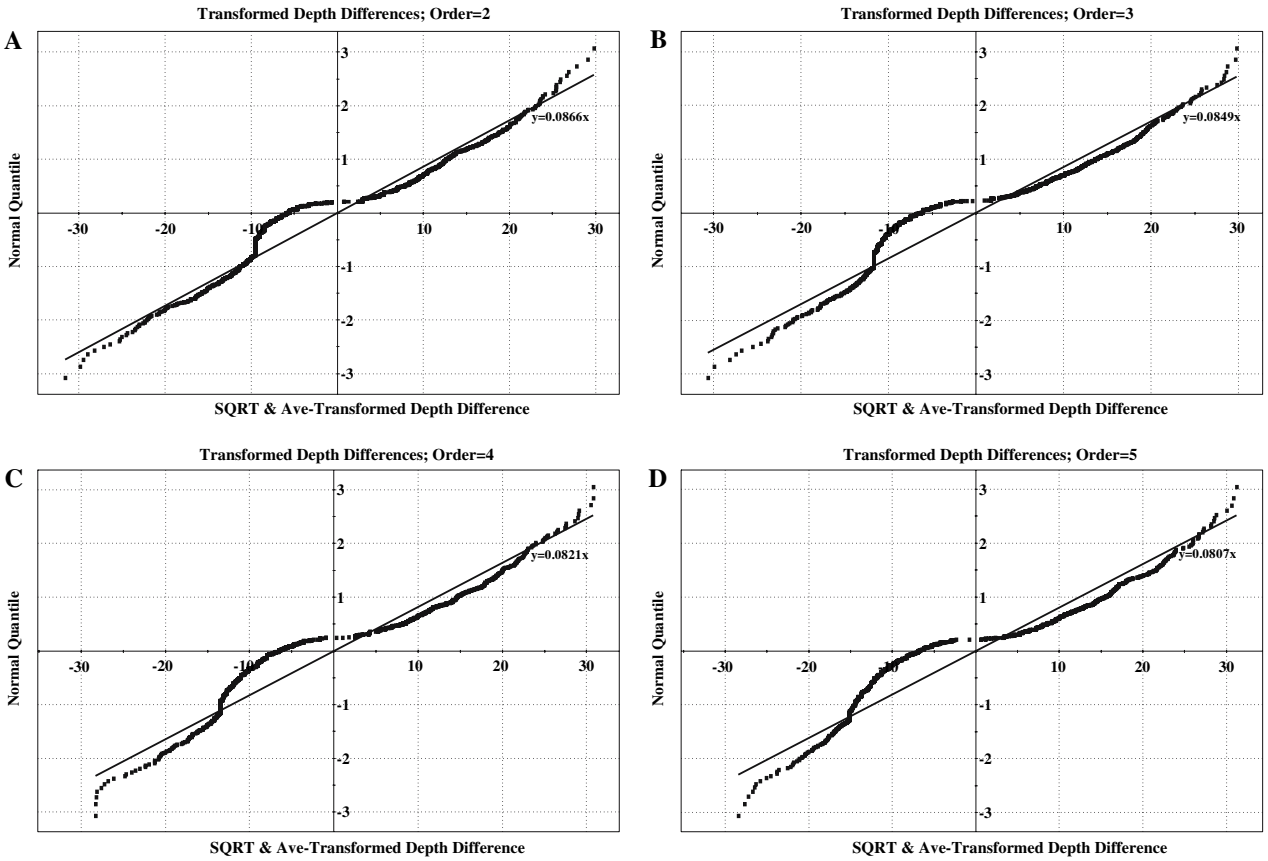

Figure 11. Normal Q–Q plots of second to fifth-order square root transformed depth differences for data set (A).

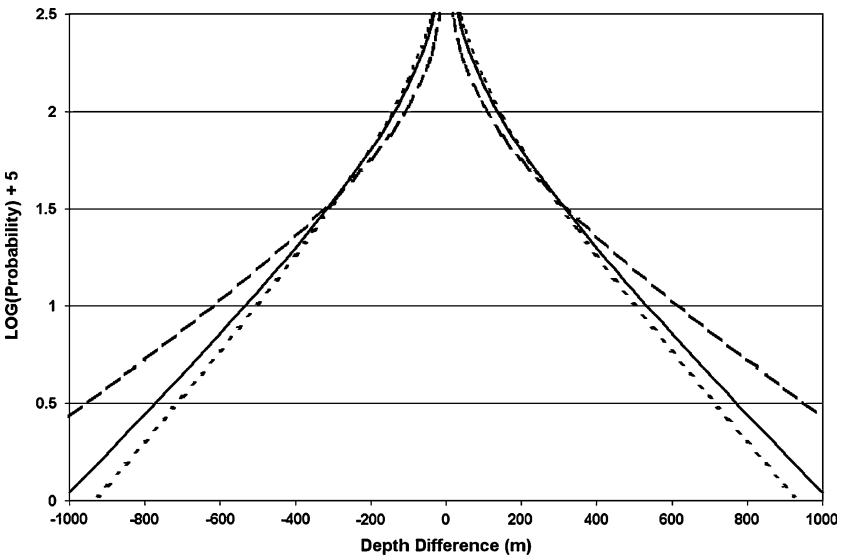

Figure 12. Double gamma frequency density curves satisfying Equation (1) with parameters derived from slope estimates of straightlines shown in Figure 8. Solid, broken, and dotted lines are for data sets (A), (B), and (C), respectively.

observed depths as such cannot be used for scaling was already recognized in the past in two ways: (1) ranking and scaling in RASC are based on superpositional relationships only, representing a reduction of observed depth differences to trinomial form; and (2) the fitting of lines of correlation (cf. Fig. 3) and subsequent variance analysis make use of relative positions of events in wells only. Along the so-called event scale (see vertical scale in Fig. 3), a unit of distance can either represent a relatively short or a relatively long interval between successive samples with observed events.

Further research and development will be performed to see whether (1) the square-root transformation of average-corrected depth differences can lead to improved scaling in RASC, and (2) the new approach can result in improved error bar estimation in CASC.

ACKNOWLEDGMENT

Thanks to Eric Grunsky, Geological Survey of Canada, for helpful suggestions.

REFERENCES

Agterberg, F. P., 1990, Automated stratigraphic correlation: Elsevier, Amsterdam, 424 p.

Agterberg, F. P., and Gradstein, F. M., 1988, Recent developments in quantitative stratigraphy: Earth Sci. Rev., v. 25, no. 1, p. 1–73.

Agterberg, F. P., and Gradstein, F. M., 1997, Measuring the relative importance of fossil events in quantitative stratigraphy, *in* Pawlowsky-Glahn, ed., Proc. IAMG'97, CIMNE, Barcelona, Part 1, p. 349–354.

Agterberg, F. P., and Gradstein, F. M., 1999, The RASC method for ranking and scaling of biostratigraphic events: Earth Sci. Rev., v. 46, no. 1, p. 1–25.

Agterberg, F. P., Gradstein, F. M., and Cheng, Q., 1998, Stratigraphic correlation on the basis of fossil events, *in* Buccianti, A. and others, eds., Proc. 4th Ann. Conf. Intern. Assoc. Math. Geology, Ischia, p. 743–748.

Agterberg, F. P., Gradstein, F. M., and Cheng, Q., 2001, RASC and CASC: Biostratigraphic zonation and correlation software, version 18: F. Agterberg, 490 Hillcrest Ave, Ottawa, K2A2M7, Canada.

Agterberg, F. P., and Nel, L. D., 1982, Algorithms for the ranking of stratigraphic events: Comput. Geosci., v. 8, no. 1, p. 69–90.

Agterberg, F. P., and Nel, L. D., 1982, Algorithms for the scaling of stratigraphic events: Comput. Geosci., v. 8, no. 2, p. 163–189.

Agterberg, F. P., Nel, L. D., Lew, S. N., Heller, M., Gradstein, W. S., D'Iorio, M. A., Gillis, D., and Huang, Z., 1989, Program RASC (Ranking and Scaling) version 12, Communic. Quantitative Stratigraphy: Bedford Institute Oceanography, Dartmouth, N.S., Canada.

Agterberg, F. P., Oliver, J., Lew, S. N., Gradstein, F. M., and Williamson, M. A., 1985, CASC FORTRAN IV interactive computer program for correlation and scaling in time of biostratigraphic events: Geol. Survey Canada, Open-File Rept. 1179.

D'Iorio, M. A., and Agterberg, F. P., 1989, Marker event identification technique and correlation of Cenozoic biozones on the Labrador Shelf and Grand Banks: Can. Petroleum Geol. Bull., v. 37, p. 346–357.

Gradstein, F. M., and Agterberg, F. P., 1982, Models of Cenozoic foraminiferal stratigraphy – northwestern Atlantic margin, *in* Cubitt, J. M., and Reyment, R. A., eds., Quantitative Stratigraphic Correlation: JohnWiley & Sons, New York, p. 119–173.

Gradstein, F. M., and Agterberg, F. P., 1998, Uncertainty in stratigraphic correlation, *in* Gradstein, F. M., and others, eds., Sequence Stratigraphy – Concepts and Applications: Elsevier, Amsterdam, p. 9–29.

Gradstein, F. M., Agterberg, F. P., Brower, J. C., and Schwarzacher, W., 1985, Quantitative stratigraphy: Reidel, Dordrecht and UNESCO, Paris, 598 p.

Gradstein, F. M., and Bäckström, S. A., 1996, Cainozoic biostratigraphy and palaeobathymetry, northern North Sea and Haltenbanken: Norsk. Geologisk. Tidsskrift., v. 76, p. 3–32.

Gradstein, F. M., Huang, Z., Merrett, D., and Ogg, J. G., 1992, Probabilistic zonation of Early Cretaceous microfossil sequences, Atlantic and Indian Oceans, with special reference top ODP Leg 123, *in* Proc. Ocean Drilling Project, Scientific Results, Leg 123, p. 759–777.

Gradstein, F. M., Kaminski, M. A., Berggren, W. A., Kristiansen, I. L., and D'Iorio, M. A., 1994, Cainozoic Biostratigraphy of the North Sea and Labrador Shelf: Micropalology, v. 40, no. Supplement, p. 1–152.

Hay, W. W., 1972, Probabilistic stratigraphy: Eclogae Geol. Helv., v. 65, p. 255–266.

Kaminski, M. A., and Gradstein, F. M., 2005, Atlas of paleogene cosmopolitan deep-water agglutinated Foraminifera, Grzybowski Foundation Spec: Drukarnia Narodowa, Kraków, Publ. no. 10, 548 p.

Liu, G., Cheng, Q., and Agterberg, F. P., in press, Design and application of graphic module for RASC/CASC quantitative stratigraphic software: Proc. IAMG-2007, Ann. l Conf. Intern. Assoc. Math. Geol. (Beijing).

Pawlowsky-Glahn, V., and Egozcue, J. J., 2001, Scaling stratigraphic events using extreme occurrences: Intern. Statistical Inst. Bull., Book 2, p. 473–476.

Schioeler, P., and Wilson, G. J., 1993, Maastrichtian dinoflagellates zonation in the Dan Field, Danish North Sea: Rev. Palaeobot. Palynol., v. 78, p. 321–351.

Van Buggenum, J. M., 1991, The range chart method: an approach toward the creation of range chart for biostratigraphic events: Géologie Africaine, Coll. Géol. Libreville, Recueil des Communic. 6–8 May 1991, p. 181–187.

Whang, P., and Zhou, D., 1997, The application of RASC/CASC methods to quantitative biostratigraphic correlation of Neogene in northern South China Sea, *in* Naiwen, W., and Remane, J., eds., Proc. 30th Intern. Geol. Congr.: v. 1. Beijing, China, VSP, Zeist.

Williamson, M. A., 1987, Quantitative biozonation of the Late Jurassic and Early Cretaceous of the East Newfoundland Basin: Micropalology, v. 33, no. 1, p. 37–65.